ICES Journal of Marine Science

ICES Journal of Marine Science (2016), 73(1), 57–74. doi:10.1093/icesjms/fsv169

Contribution to the Symposium: '*International Eel Symposium 2014*'

Original Articles

Exploring the role of the physical marine environment in silver eel migrations using a biophysical particle tracking model

Mélanie Béguer-Pon[1,2]*, Shiliang Shan[2], Keith R. Thompson[2], Martin Castonguay[3], Jinyu Sheng[2], and Julian J. Dodson[1]

[1]*Département de Biologie, Université Laval, Pavillon Vachon, 1045 avenue de la Médecine, QC, Canada G1V 0A6*
[2]*Department of Oceanography, Dalhousie University, 1355 Oxford Street, PO Box 15000, Halifax, NS, Canada B3H 4R2*
[3]*Institut Maurice-Lamontagne, Pêches et Océans Canada, 850 route de la Mer, C.P. 1000, Mont-Joli, QC, Canada G5H 3Z4*

**Corresponding author: e-mail: melanie.beguer@dal.ca*

Béguer-Pon, M., Shan, S., Thompson, K. R., Castonguay, M., Sheng, J., and Dodson, J. J. Exploring the role of the physical marine environment in silver eel migrations using a biophysical particle tracking model. – ICES Journal of Marine Science, 73: 57–74.

Received 1 December 2014; revised 8 September 2015; accepted 13 September 2015; advance access publication 11 October 2015.

Both the American eel (*Anguilla rostrata*) and European eel (*Anguilla anguilla*) undertake long-distance migrations from continental waters to their spawning sites in the Sargasso Sea. Their migration routes and orientation mechanisms remain a mystery. A biophysical particle tracking model was used in this study to simulate their oceanic migration from two release areas: off the Scotian Shelf (Canada) and off the Irish continental shelf. Two plausible swimming-directed behaviours were considered for simulating two different migratory paths: true navigation to specific spawning sites and innate compass orientation towards the vast spawning area. Several combinations of swimming speeds and depths were tested to assess the effect of ocean circulation on resulting migratory pathways of virtual eels (v-eels), environmental conditions experienced along their oceanic migration, and energy consumption. Simulations show that the spawning area can be reached in time by constantly swimming and following a readjusted heading (true navigation) or a constant heading (compass orientation) even at the lowest swimming speed tested (0.2 m s^{-1}) for most v-eels. True navigation might not be necessary to reach the spawning area. The ocean currents affect mainly the migration of American v-eels, particularly for swimming speeds lower than 0.8 m s^{-1}. The ocean circulation increases the variability in the oceanic migration and generally reduces the efficiency of the v-eels, although positive effects can be possible for certain individuals. The depth range of diel vertical migration (DVM) significantly affects the total energy expenditure due to the water temperature experienced at the various depths. Model results also suggest that energy would not be a limiting factor as v-eels constantly swimming at 0.8 BL s^{-1} spent <25 and 42% of energy available for migration for American and European v-eels, respectively.

Keywords: anguillid eels, animal orientation and navigation, energy, modelling, NEMO, particle tracking, spawning oceanic migration.

Introduction

Both the American and European eels are panmictic and facultatively catadromous species which spawn in the Sargasso Sea from February to mid-July (McCleave *et al.*, 1987; McCleave, 2003). After decades of research, the long-distance oceanic migration of these species from coastal and continental waters to the Sargasso Sea still remains unknown (Tesch, 2003). Although the spawning sites, which cover a vast area of more than 1.7×10^6 km^2, have been inferred from the collection of leptocephalus larvae during several expeditions (Schmidt, 1923; McCleave, 2003; Miller *et al.*, 2015), no adults have ever been caught in the open ocean. Knowledge is very limited about the migratory path, the location of the spawning sites, the navigation/orientation cues eels use, and the environmental conditions which they experience. Filling this knowledge gap is crucial for research and management purposes, especially considering the precarious status of both species. The European eel is listed as critically endangered on the IUCN red list (Jacoby and Gollock, 2014), whereas the American eel is listed as endangered on the same list (IUCN, 2014) and as threatened in Canada (COSEWIC, 2012). Good understanding of the routes silver eels take, and the cues they use, will also allow reliable prediction of migratory routes under various climate change scenarios and the impact of such changes on these species.

Over the past decade, technological developments, particularly in the area of miniaturized pop-up archival satellite tags, have allowed the tracking of eels during the early phase of their marine migration (e.g. Aarestrup *et al.*, 2009). Limited but useful information about the silver eel behaviour in the ocean has been collected. For example, marked diel vertical migrations (DVMs) appear to be a common behaviour among anguillid species (Aarestrup *et al.*, 2009; Manabe *et al.*, 2011; Beguer-Pon *et al.*, 2012; Schabetsberger *et al.*, 2013). Recently, silver European eels were tracked for up to 2300 km from the Swedish coast to the north of Ireland (Westerberg *et al.*, 2014), providing insights into the eel trajectories and orientation behaviour during the early phase of their marine migration. Nevertheless, as in other similar studies (Beguer-Pon *et al.*, 2012; Wahlberg *et al.*, 2014), eels were not tracked during the full oceanic migration. The closest pop-up location of the satellite tags was more than ca. 3700 km from the Sargasso Sea spawning site for European eels (Aarestrup *et al.*, 2009). Satellite tags, however, are not without potential shortcomings. They could impact the swimming performance of the tracked eels (as demonstrated in laboratory studies, e.g. Methling *et al.*, 2011) and exacerbate the predation risk at sea (e.g. Beguer-Pon *et al.*, 2012).

The means by which eels navigate or orientate in the ocean are currently unknown. Unlike piloting, a fish using compass orientation or true navigation reaches its destination without reference to local landmarks and moves over unfamiliar territory in a new and unfamiliar direction. For compass orientation, the designed area can be reached only when the compass direction leads to home or a familiar area. For true navigation, the destination is reached by using information available at the point of departure independently of the outward journey and the migrant uses a bicoordinate map involving at least two large fields of gradients that are established by extrapolation of home-site conditions (e.g. Dodson, 1988). Among the hypothetical cues that could allow eels to cross the Atlantic Ocean in the absence of familiar landmarks, the Earth's magnetic field appears to be the principal hypothesis permitting compass orientation and navigation (Tesch, 2003; Durif *et al.*, 2013). It has been known for a long time that eels have sufficient sensitivity to detect existing environmental magnetic fields (e.g. Tesch, 1974; Souza *et al.*, 1988; Tesch *et al.*, 1992). Recent laboratory experiments conducted on European eels supported the conclusion that eels have a magnetic compass and they use this sense to orientate themselves in a direction previously recorded before their displacement (Durif *et al.*, 2013). Putman *et al.* (2014) showed that juvenile Pacific salmon use a combination of magnetic intensity and inclination angle to assess their geographic locations. These studies imply that magnetic maps are inherited and they are phylogenetically widespread, which likely explain the extraordinary navigational abilities evident in many long-distance oceanic migrants. Ocean currents, i.e. drift, could also provide the degree of directional bias necessary to explain a part of the migration (Dodson, 1988; Fricke and Kaese, 1995). The movement of eels resulting from the combined effect of the water currents and the eel's own propulsion may significantly contribute to their progress, but the currents could provide either significant hindrance or assistance, or produce lateral displacement (Chapman *et al.*, 2011). Assessing the role of currents during the silver eel's oceanic migration hence appears to be potentially very important, but it has never been quantified. It is also unclear how much time it takes for eels to get to their spawning sites. Therefore, it is crucial to take into account the effect of currents for calculating the duration of migration. For instance, without any ocean currents, an eel leaving the coast of Nova Scotia would have a transit great-circle distance (i.e. shortest distance between two points on the surface of Earth) of ca. 2750 km to reach the assumed spawning sites. The transit time is ca. 40 d under a sustained swimming speed of 0.8 m s^{-1}. Similarly, the transit time for a European eel departing the coast of Ireland would be ca. 72 d with a transit distance of ca. 5000 km. The above calculation suggests that transit times are well within the estimated spawning time windows, but the marine environment has strong spatial and temporal variability (e.g. the Gulf Stream) so we may thus ask if the above estimates are reasonable. The other important questions to be addressed include "What is the effect of the oceanic circulation on the migratory pathway of silver eels?" and "How does the physical environment affect energy expenditure during the spawning migration (e.g. Boëtius and Boëtius, 1980; van den Thillart and van Ginneken, 2007)?"

Although numerical models are potentially useful for addressing such questions about silver eel oceanic migration, to our knowledge, only one numerical study was conducted in the past using biophysical particle tracking experiments (Fricke and Kaese, 1995). In their study, Fricke and Kaese (1995) simulated the migration of European eels by releasing particles off the European coasts swimming at around 200 m depth at a constant heading to the southwest. The authors estimated the duration of migration according to their fixed parameters and concluded that ocean currents may play an important role. The horizontal resolution of the flow field used in their study was $(1/3)^\circ$ and Fricke and Kaese (1995) assumed that eels swam at only one depth, whereas it is now well established that eels undergo marked DVM (up to ca. 1.2 km in depth; e.g. Aarestrup *et al.*, 2009; Wysujack *et al.*, 2015).

In this study, we used a particle tracking model which incorporates directed swimming movements to simulate the migration of adult American and European eels from the coastal and shelf waters to the Sargasso Sea. Both species were considered since they reproduce in the same general area at the approximately same time and probably use the similar orientation/navigation behaviours to reach the spawning sites (McCleave *et al.*, 1987). The main objectives of our study were to simulate their oceanic migration using two different, directed swimming behaviours: true navigation towards the spawning area and innate compass orientation towards the Sargasso Sea and to assess the effect of the flow field on the resulting migratory patterns (duration of migration, trajectories, environmental conditions experienced along the way, and energy expenditure). Several combinations of different swimming speeds and swimming depths were examined.

Material and methods

The biophysical particle tracking

Particle tracking models are increasingly being used in investigating the transport pathways, mixing, residence time and hydrodynamic connectivity in the ocean (e.g. Ridderinkhof and Zimmerman, 1990; Bilgili *et al.*, 2005; Shan and Sheng, 2012). The orientated swimming of marine animals adds a layer of complexity to the particle tracking model. To accommodate this, a particle tracking model was developed in MATLAB® to include the ocean components (currents, salinity, and temperature) and various migratory behaviours. In this study, the three-dimensional ocean currents used to drive the particle tracking model were

produced by a time-varying eddy-permitting model of the North Atlantic. Positions of each virtual eel (v-eel) were tracked in a quasi three-dimensional fashion to include DVM. The oceanic temperature, salinity, and energy expenditure were also calculated along the migration route.

The movement of v-eels can be expressed in terms of the physical and biological components:

$$\frac{\mathrm{d}\vec{x}}{\mathrm{d}t} = \vec{u}_p(\vec{x}, t) + \vec{u}_b(\vec{x}, t), \quad (1)$$

where $\vec{x}$ is the eel position at time t, $\vec{u}_p$ and $\vec{u}_b$ are the components of flow associated with passive drift by ocean currents and active migratory swimming, respectively. Both $\vec{u}_p$ and $\vec{u}_b$ are functions of space and time. A forward Euler time-stepping scheme was used to solve Equation (1).

Physical component ($\vec{u}_p$)

The time-dependent three-dimensional circulation over the North Atlantic was produced by an ocean general circulation model, which was developed during the GOAPP project (Global Ocean-Atmosphere Prediction and Predictability, http://www.goapp.ca/) and used to study the circulation of the North Atlantic (Higginson *et al.*, 2011; Higginson, 2012). The model is based on version 2.3 of NEMO (Nucleus for European Models of the Ocean) with the OPA (Océan PArallélisé) ocean component (Madec, 2008). The model grid covers the North Atlantic (5–68°N, 100°W–34°E, Figure 1) with a nominal (1/4)° horizontal resolution and a maximum of 46 levels in the vertical. The model forcing at the sea surface, including wind stress, net heat fluxes, and freshwaters, was specified using the CORE (Common Ocean-ice Reference Experiments) normal-year dataset. The lateral boundary conditions were specified using temperature, salinity, and transport obtained from a global (1/4)° model. To suppress drift and bias, the model was spectrally nudged (Thompson *et al.*, 2006) to a monthly temperature and salinity climatology constructed from a blend between the Yashayaev climatology (http://www2.mar.dfo-mpo.gc.ca/science/ocean/woce/climatology/naclimatology.htm) and the PHC (Polar science center Hydrographic Climatology)/Levitus climatology (Steele *et al.*, 2001). The model was integrated for 16 years from January 1990 to December 2005, and model simulations of three-dimensional currents, temperature and salinity were stored every 5 d. The 2004 and 2005 model results were used to provide three-dimensional ocean currents and hydrographic fields over the North Atlantic. A nearest-neighbour-based scheme is used to interpolate the modelled currents, temperature, and salinity to the particle location.

The ocean circulation in the North Atlantic has been the subject of many studies over the past century (see Schmitz and McCartney, 1993 for a review). The subtropical and subpolar gyres have been identified and studied (e.g. Reid, 1994; Talley *et al.*, 2011). In the following paragraph, a brief summary of the circulation system in the North Atlantic is provided. The major upper ocean circulation pattern in the North Atlantic consists of the subtropical and subpolar gyres (Figure 1b and c). The dominant feature of the North Atlantic circulation in the upper layer is the Gulf Stream (GS). The current is energetic, exceeding 1 m s^{-1} in places, and the water is relatively warm and saline. Near Cape Hatteras, the GS moves offshore into deeper waters and the path becomes more variable with meanders and eddies. Beyond the tail of the Grand Banks, the GS becomes the North Atlantic Current (NAC). Part of the NAC separates to form the Azores Current.

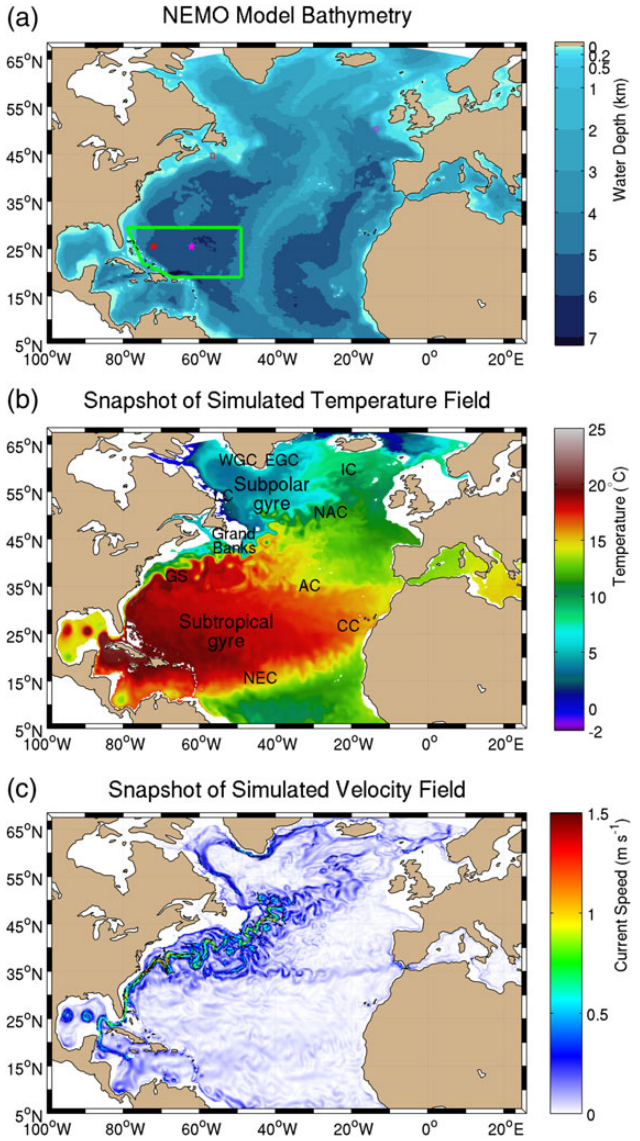

Figure 1. The North Atlantic Ocean model (a) bathymetry and snapshot of simulated (b) temperatures (°C) and (c) velocity field (m s^{-1}) at 200 m at the end of October 2004. In (a), areas marked by the red and magenta boxes indicate the initial release locations of the American and European eels, respectively. The area marked by the green polygon indicates the assumed spawning area. The red (72°W, 25.5°N) and magenta (62°W, 25.5°N) stars indicate the locations where the smallest American and European eel larvae were found, respectively. In (b), the currents that are labelled are the Gulf Stream (GS), the North Atlantic Current (NAC), the Azores Current (AC), the Canaries Current (CC), the North Equatorial Current (NEC), the Irminger Current (IC), the East Greenland Current (EGC), the West Greenland Current (WGC), and the Labrador Current (LC). In (c), the current direction for the current speed >0.2 m s^{-1} is indicated by the black arrows.

The latter flows eastward and feeds recirculations to the south and west, such as the Canaries Current and the North Equatorial Current, completing the circulation that is the subtropical gyre. The remainder of the NAC continues northeastwards, either towards the Norwegian Sea or into the subpolar gyre. This gyre comprises the Irminger Current towards Iceland, with return

flow equatorward via the East and West Greenland and Labrador currents.

The three-dimensional physical flow simulated by the NEMO model reproduces reasonably well the subtropical and subpolar circulation, in terms of both long-term mean and temporal variability (Supplementary Figure S1). The GS extension is one of the energetic regions in the North Atlantic. The modelled temperature field features warm and cold core rings near the confluence regime of GS and Labrador Current (Figure 1b). The circulation model also captures the separation of the GS and the relatively strong mesoscale variability in the GS extension region (Supplementary Figure S1).

A random walk process was included in the particle tracking model to account for the particle movement associated with subgrid-scale turbulence and other local processes which are not resolved by the circulation model. The random displacement at each time-step of the model is defined by: $\xi\sqrt{2K\Delta t}$, where ξ is a Gaussian random variable with zero mean and unit variance, K the horizontal eddy diffusivity coefficient, and Δt the time-step (Taylor, 1922). Based on sensitivity studies, K is set to be homogeneous and isotropic with a value of 10 $m^2\ s^{-1}$ (Riddle and Lewis, 2000).

Biological component ($\vec{u}_b$)

The biological component $\vec{u}_b$ was modelled probabilistically using a Multiple Response Movement Model. The idea is to express the probability density of the swimming velocity at a given time as a mixture distribution:

$$p(\vec{u}_b) = \sum_{i=1}^{m} \alpha_i\, p_i(\vec{u}_b), \tag{2}$$

where p_i is the biological velocity probability distribution for the ith behavioural preference. The weighting factors (α_i) determine the relative importance of the ith swimming response at a given time. It should be noted the probability density function $p(\vec{u}_b)$ is a weighted sum of the individual components with $\sum_{i=1}^{m} \alpha_i = 1$ and $0 \leq \alpha_i \leq 1$. In this study, two responses ($m = 2$) of swimming behaviours were implemented: random searching ($i = 1$) and directed swimming ($i = 2$). A detailed description of the preferred directed swimming is given in the following section.

Simulated eel swimming behaviours

Horizontal behaviour

Silver eels do not feed while migrating (Tesch, 2003). A passive drift was first examined (Exp_{drift}, Table 1) in which the v-eels are transported by ocean currents without active horizontal swimming behaviours. Three active swimming behaviours were evaluated following three experiments (Table 1): (i) random swimming (Exp_{rand}), (ii) true navigation towards a target (core spawning area) in the Sargasso Sea (Exp_{Navi}), and (iii) innate compass orientation towards the boundaries of the spawning area in the Sargasso Sea (Exp_{Ori}). In Exp_{rand} ($\alpha_1 = 1$, i.e. 100% of the swimming effort is directed towards random searching), each v-eel randomly selects a direction at each time-step regardless of the oceanic current direction or the eel's position. Mathematically, the distribution of swimming direction [$\boldsymbol{p}(\boldsymbol{\theta})$] follows a uniform distribution from 0° to 360° [$\boldsymbol{p}(\boldsymbol{\theta}) = \mathbf{U}(\mathbf{0}^\circ, \mathbf{360}^\circ)$]. The other two active behaviours have preferred swimming directions ($\boldsymbol{\theta_0}$). The swimming direction at each time-step is sampled from a weighted sum of two uniform distributions with 90% effort drawn from a preferred directed swimming centred on $\boldsymbol{\theta_0}$ and 10% effort associated with random searching:

$$\boldsymbol{p}(\boldsymbol{\theta}) = 0.9\mathbf{U}(\boldsymbol{\theta}_0 - \boldsymbol{\Delta\theta}, \boldsymbol{\theta}_0 + \boldsymbol{\Delta\theta}) + \mathbf{0.1U}(\mathbf{0}^\circ, \mathbf{360}^\circ)\,, \tag{3}$$

where $\boldsymbol{\Delta\theta}$ represents the spread around the preferred direction. In this study, we set $\boldsymbol{\Delta\theta} = \mathbf{22.5}^\circ$. The main purpose for implementing some random searching and a spread is to account for other unresolved biological behaviours and environmental distractions during the eel's migration.

For the true navigation (Exp_{Navi}), the preferred swimming direction ($\boldsymbol{\theta_0}$) is directed towards the spawning site and $\boldsymbol{\theta_0}$ is adjusted at each time-step according to the v-eel's current position and the spawning site. This swimming behaviour assumes that eels possess an internal map of the Earth's geomagnetic field and have knowledge of the location of the general spawning area. For the compass orientation behaviour towards the Sargasso Sea (Exp_{Ori}), the preferred swimming direction ($\boldsymbol{\theta_0}$) is fixed and not adjusted at each time-step. The heading is fixed at 180°T (i.e. to the south) and 217.7°T (southwest) for American eel and European eel, respectively. In this latter behaviour, eels migrate towards the boundaries of the spawning area using an innate compass direction. Other orientation mechanism(s) that would allow them to reach the exact location of the spawning site within the Sargasso Sea are not simulated. Therefore, only the success in reaching the boundaries of the spawning area is calculated for this behaviour (see below).

Diel vertical migration

The DVMs have been observed for both eel species at sea (Aarestrup *et al.*, 2009; Beguer-Pon *et al.*, 2012; Westerberg *et al.*, 2014), in which eels remain in relatively shallow water at night, while at dawn they make a steep dive to deep waters (up to 1200 m) where they remain for the day before ascending again at dusk. We implemented DVM in our experiments with four vertical specific layers: 50 and 200 m as "surface" layers experienced at night, and 600 and 1000 m as "deep" layers experienced during the day. Four combinations of vertical migrations were tested: 50–600, 200–600, 50–1000, and 200–1000 m. In this study, an equal duration of night and day was assumed, which means that a 12-h alternation between surface and deep layers was achieved in the particle tracking model by shifting v-eel's vertical position from one layer to the other layer instantaneously. In reality, however, the duration of night and day is not equal, and changes as the eels migrate to the Sargasso Sea by way of seasonal daylight changes and local effects on daylength. We also assume v-eels perform horizontal swimming continuously day and night. The particle tracking experiments with various behaviours are listed in Table 1.

Table 1. List of tested horizontal swimming behaviours.

Experiments	Migratory behaviours	Description
Exp_{Drift}	Passive drift	No swimming. Carried by ocean currents
Exp_{Rand}	Random direction	Swimming in random direction
Exp_{Navi}	True navigation	Constantly adjust to the spawning area
Exp_{Ori}	Compass orientation towards the Sargasso Sea	South (180°T) for American v-eel, southwest (217.7°T) for European v-eel

The heading units are degrees from true north in a clockwise direction (North is 0°T and south is 180°T).

Key biological parameters of eels used in the model

In this study, we chose three body lengths (Total length, TL) that correspond to the smallest (ca. 40 cm), the mean size (ca. 64 cm), and the largest (ca. 101 cm) silver eels that are usually caught during their downstream migration in Europe and in North America at latitudes that cover the departure location chosen for our simulations (Vollestad, 1992; Jessop, 2010). The largest eels correspond to females (Krueger and Oliveira, 1997). Four swimming speeds were also examined in simulations, ranging from a low value (0.5 BL s^{-1}) to a high value (1.5 BL s^{-1}) (Table 2). These speed values were used in swim tunnel experiments on male and female European eels. and the optimal speed at 18°C was estimated at between 0.7 and 1.0 BL s^{-1} (van den Thillart and van Ginneken, 2007; Burgerhout *et al.*, 2013a, b).

Energy expenditure

The initial energy reserve (E_i) was calculated using the total amount of protein and lipid content which are ~17 and 21% of the body mass (M_0), respectively, based on eels caught in Lake Ontario in 2008, P. Hodson, Queens University; pers. comm.). In the calculation, we used the energy equivalents 2.4×10^4 J g^{-1} for protein and 4.0×10^4 J g^{-1} for fat [Kleiber, 1975 in Lambert and Dodson (1990)], i.e. $E_i = 12\,480\ M_0$ (J). According to Palstra *et al.* (2006, 2010), around 28% of the total fat reserve was used for gonad maturation, implying that $E_M = 2352\ M_0$ (J) are kept for maturation. We also arbitrarily assumed that 20% of the energy reserves is dedicated for survival and thus not available for swimming. The reproductive reserve is removed before the survival component was calculated. Consequently, the initial energy reserve available for transportation for each v-eel was $E_0 = 8102\ M_0$ (J). The body mass (M_0) was assessed using the formula available in Tesch (2003) for silver European eels ($M_0 = 6e^{-7}TL^{3.1803}$) and the formula of Owens and Geer (2003) for silver American eels ($M_0 = 4e^{-7}TL^{3.2618}$). At each time-step of calculation, the cost of migration (E_T) was calculated according to an empirical formula based on a literature review of laboratory experiments that investigated the oxygen consumption of eels as a function of swimming speeds (van den Thillart and van Ginneken, 2007; Methling *et al.*, 2011), water temperature (Walsh *et al.*, 1983), and body mass (Degani *et al.*, 1989; Clarke and Johnston, 1999). The energy conversion factor for respirometry of 18.89 J ml^{-1} O_2 (Elliott and Davison, 1975; van Ginneken *et al.*, 2005) was used to obtain the corresponding energy in joules. Details about the procedure to obtain the final formula for calculating the energetic cost of transport can be found in the Supplementary material (Protocol 1S). The final formula is given as:

$$\Delta E_t = 0.7 \times 10^{-3}(96.62V_t^{2.51} + 0.140256MR_t^{0.79}C_T)\Delta t \times 18.89, \quad (4)$$

where V_t is the swimming speed (in BL s^{-1}) at time t, MR_t the remaining body mass (in g) at time t, and C_T a coefficient that takes into account the effect of water temperature on the oxygen consumption rate. The coefficient C_T has three values: 0.5, 1, and 1.6 for temperature below 7.5°C, between 7.6 and 15°C and above 15°C, respectively.

Design of particle tracking experiments

The v-eels were released over two 1 × 1° areas which are separated from each other. One release area was over the Scotian Shelf off the Laurentian Channel in Canada for the American eel, and the other was over the Irish continental shelf for the European eel

Table 2. Number of scenarios (numerical experiments) conducted with different combinations of parameters.

	Ocean currents (NEMO 2004–2005)		(α_1, α_2)		Body length (BL, mm)			Swimming speed (BL s^{-1})				DVM (Top/bottom, m)				Total runs for both species
Values	On	Off	(1.0, 0.0)	(0.1, 0.9)	404	637	1016	0.5	0.8	1.0	1.5	50/600	50/1000	200/600	200/1000	
Exp_{Drift}	✓				✓									✓		2
Exp_{Rand}	✓		✓		✓				✓					✓		2
Exp_{Navi}	✓	✓		✓	✓	✓	✓	✓	✓	✓	✓	✓	✓	✓	✓	192
Exp_{Orie}	✓	✓		✓	✓	✓	✓	✓	✓	✓	✓	✓	✓	✓	✓	192
Total number of scenarios																388

Here α_1 is the weighting factor of the random swimming response, while α_2 is the weighting factor of the preferred direction swimming response [Equation (3)].

(Figure 1a). The Scotian Shelf was chosen because of the potential importance of migrating silver eels from the St. Lawrence system (largest individuals, majority of females, Jessop, 2010) and the Irish continental shelf corresponds to areas where satellite tracking studies of eels started or ended (Aarestrup *et al.*, 2009; Westerberg *et al.*, 2014). The spawning area was defined according to Miller *et al.* (2015). In Exp_{Navi}, a target inside the spawning area was assigned for each species (Figures 1 and 2). Each target represents the most probable site according to empirical distribution data for the smallest larvae (Kleckner and McCleave, 1985; Miller *et al.*, 2015) and supported by the recent modelling work of Rypina *et al.* (2014) for the American eel. Most silver eels exiting from their freshwater growth habitats are caught from June to January for both species (e.g. Helfman *et al.*, 1987; Davidsen *et al.*, 2011; Verreault *et al.*, 2012; MacNamara and McCarthy, 2013). For each particle tracking experiment, six successive releases of a patch of 500 particles were performed, at a 5 d interval, over a period of the migration-departure time window (the month of November for American eels and December for European eels; 6 releases; Figure 1a). This suppresses the dependence of numerical results on the release time. The positions of 3000 v-eels (500 particles × 6 releases) were updated using Equation (1) and tracked for a period of 250 d with a time-step of 3 h for each species. A total of 388 scenarios were considered with a different combination of parameters (Table 2). Success was defined as the percentage of particles reaching the boundaries of the global spawning area (all behaviours) and also reaching the specific target within spawning areas (most probable or core spawning site; Exp_{Navi} only). The great-circle distance between the northern boundary of the global spawning area and the specific target within it is ca. 630 km for American eels and 520 km for European eels. The success rate was calculated at the beginning and end of the spawning season, which are after 107 and 180 d of tracking, respectively, for American eels (mid-February/March and late May), or after 150 and 250 d of tracking, respectively, for European eels (March and late July; Miller *et al.*, 2015). At each model time-step (i.e. every 3 h), the following four key variables were calculated and stored: the oceanic currents, the water temperature, the salinity, and the eel's energy consumption. For each eel species, the ensemble means of these variables from the 3000 particles were calculated for each scenario. It is known that the tracking results could be sensitive to the number of particles released. A sensitivity study was thus conducted on the number of particles required to achieve statistically stable results. The results suggest that the estimation of success rate is not reliable for the number of particles of <100 and converge for the number of particles >400 (Supplementary Figure S2). In consideration of the

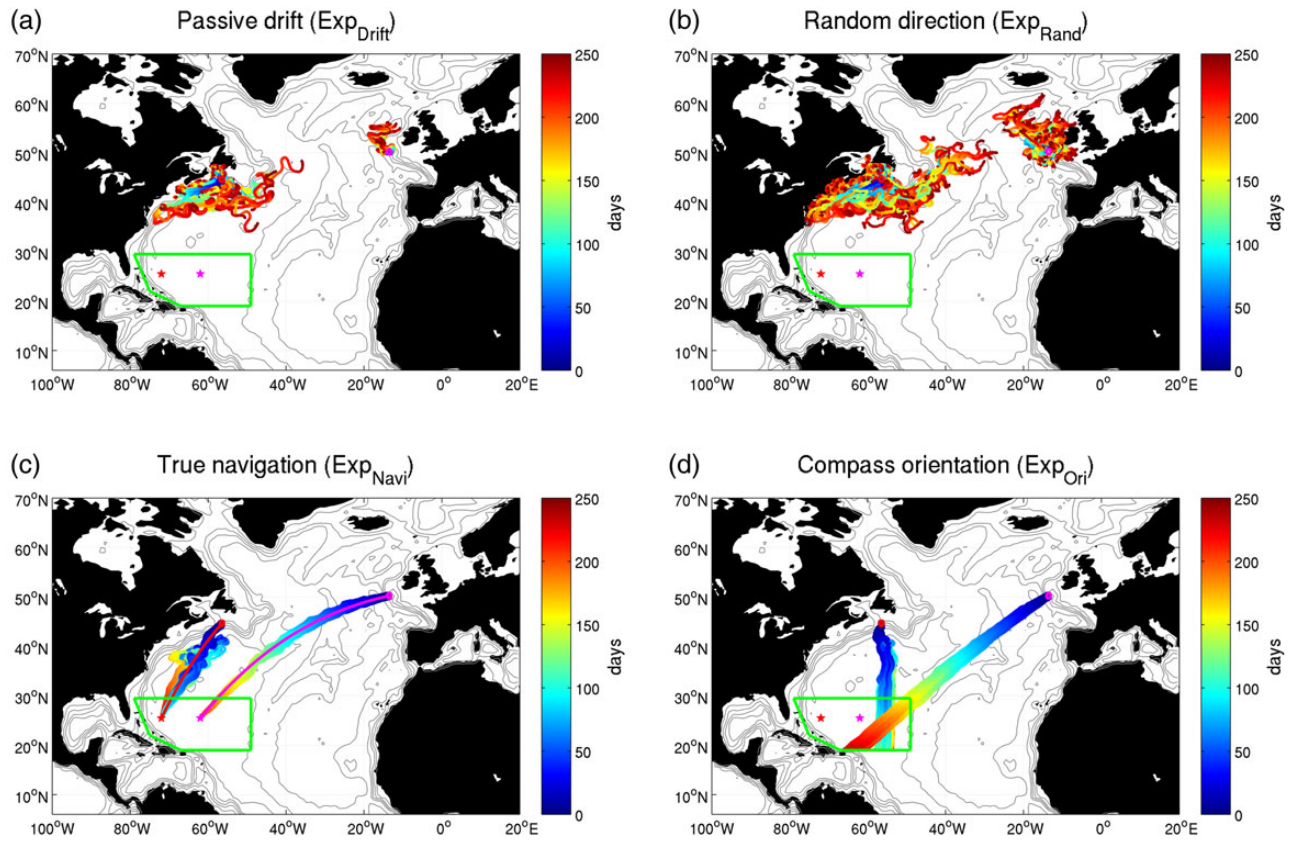

Figure 2. Selected v-eel trajectories from four particle tracking experiments (Table 1): (a) Passive drift, (b) Random direction, (c) True navigation and (d) Compass Orientation. The v-eels had a body length of 404 mm, a swimming speed of 0.8 BL s^{-1}, and made DVMs between 200 and 600 m. In each tracking experiment, 3000 virtual eels were tracked for each species. For clarity, 1200 v-eel trajectories were randomly selected for each species and plotted. The red and magenta squares indicate the initial release areas for American and European eels, respectively. The green polygon is the spawning area in the Sargasso Sea. The red and magenta stars indicate locations where the smallest American and European eel larvae were found, respectively. The red and magenta lines connecting the squares and starts in (c) indicate v-eel trajectories without background oceanic currents, which are the great-circle (shortest) lines.

computational time required for running the 388 scenarios and the disk space needed to store the results, we chose to seed 500 particles for each release in this study (for six different times, i.e. 3000 particles for each scenario).

The particle tracking results were quantified by analysing the v-eel trajectories, success and duration of migration, energy expenditure, and environmental conditions experienced along the way. The effects of the various parameters (oceanic background current, horizontal behaviour, swimming speed, and depth range) on the success of different behavioural scenarios were statistically evaluated using generalized linear models (Bolker *et al.*, 2009). The effect of the flow field on the spawning migration was assessed by comparing the mean success, duration of migration, total distance travelled, and the energy cost of scenarios in the presence of the oceanic background current with those scenarios performed in the absence of the oceanic background current independently for the two directed swimming behaviours.

Results

Success and duration of migration

Passive drift ($\vec{u}_p$ only)

Figure 2a shows v-eel trajectories in the passive drift experiment (Exp_{Drift}). Passive v-eels released over the Scotian Shelf were first advected by currents over the shelf break. Some particles spread onto the Shelf. Some particles drifted into the open ocean then were advected by the GS to the east. After passing 50°W, some particles drifted northeastward with the NAC and some particles moved southeastward with the Azores Current. Passive v-eels released off the Irish continental shelf were advected to the northeast by the NAC ($\sim$0.3 m s^{-1} at 200 m, Figure 1c). The results in Exp_{Drift} suggest that none of the passive v-eels released either over the Scotian Shelf or the Irish continental shelf reach the Sargasso Sea after 250 d of tracking (i.e. at the end of the spawning period for European eel) for the four tested ranges of DVM (50/600, 50/1000, 200/600, 200/1000 m).

Active swimming behaviour ($\vec{u}_p + \vec{u}_b$)

Random swimming (Exp_{Rand})

The trajectories of v-eels with random swimming (Figure 2b) were mainly advected by the oceanic background flow ($\vec{u}_p$), resulting in a general pattern similar to the results of Exp_{Drift} (Figure 2a). The stochastic nature of random swimming ($\vec{u}_b$) is reflected in the "fuzziness" of each individual trajectory. For the American v-eels, a few were able to escape from the GS and move towards to the northern boundary of the spawning site after 250 d. The V-eels released off Ireland were mainly trapped in the NAC and the Irminger Current. After 250 d, they were far away from the spawning site. The results in Exp_{Rand} suggest that without a preferred swimming direction, the v-eels could not reach the spawning sites in a realistic time window.

Preferred directed swimming (Exp_{Navi} and Exp_{Ori})

Both directed swimming behaviours generally led to successful outcomes (Table 3), but the success and the duration of migration mainly depend on the swimming speed (Table 4). For American v-eels, all cases of true navigation (Exp_{Navi}) were successful, with all of the v-eels reaching the target before the beginning of the spawning season if their swimming speeds were $\geq$0.5 m s^{-1} (Figure 3). A swimming speed of 0.2 m s^{-1} allowed 49.1% of the American v-eels to reach the target before the end of the spawning season. European v-eels swimming at or faster than 0.8 m s^{-1} arrived before the beginning of the spawning season and those swimming at 0.3 m s^{-1} arrived before the end of the spawning season. V-eels swimming at 0.2 m s^{-1} did not complete the migration in time (Exp_{Navi}; Figure 4). The simulations showed that v-eels navigating towards their spawning area must swim constantly at a minimum of 0.25 m s^{-1} for American v-eels and minimum 0.3 m s^{-1} for European v-eels [i.e. 0.8 BL s^{-1} for the smallest eels (40 cm)] to reach the spawning site in time (Exp_{Navi}). On average and at the optimal swimming speed of 0.8 BL s^{-1} (van den Thillart and van Ginneken, 2007; Palstra *et al.*, 2008), small American v-eels reached the target within 103 d (range: 77–242 d), medium ones within 64 d (range: 54–162 d), and large ones within 40 d (range: 35–58 d) (Exp_{Navi}), before or at the beginning of the spawning season (Figure 3). For the same scenarios, small European v-eels reached the target at the end of their spawning season (within 206 d; range 191–224 d), the medium v-eels at the beginning of the spawning season (within 129 d; range 121–137 d) and the largest before the spawning season (within 81 d; range: 76–86 d) (Figure 4). The resulting average net ground travel speeds, which was calculated using the distance travelled

Table 3. Overall success of the tested scenarios (taking into account the oceanic circulation).

		Behaviour		
		True navigation		Orientation towards Sargasso Sea
	Species	To target inside spawning area	To limits of spawning area	To limits of spawning area
Success[a] at the beginning of the spawning season	American v-eel	87.1 (0–100)	90.2 (7.4–100)	99 (90.6–100)
	European v-eel	33.3 (0–100)	34.6 (0–100)	50 (0–100)
Success[a] at the end of the spawning season	American v-eel	94.9 (49.8–100)	96.8 (69.5–100)	100 (99.7–100)
	European v-eel	91.7 (0–100)	91.7 (0–100)	93.1 (17.6–100)
Duration of migration (d)	American v-eel	97 (19–250)	86 (15–250)	68 (15–250)
	European v-eel	119 (40–225)	106 (35–203)	99 (35–175)
Distance travelled (km)	American v-eel	3886 (2752–7160)	3391 (2294–6640)	2472 (1942–3447)
	European v-eel	5838 (5012–6949)	5208 (4420–6243)	4619 (4131–5151)
Percentage of energy spent for transportation	American v-eel	24.5 (15.5–47.7)	20.5 (12.9–40.2)	17.6 (9–35.8)
	European v-eel	44.6 (27.6–81.3)	40.4 (24.7–75.1)	34.7 (21–67.8)

Means with ranges (min–max) are reported.
[a]Percentage of particles reaching the limits of the spawning area or the target inside the spawning area.

Table 4. Results from the generalized linear model (GLM) that examined the effect of factors on the transit time (duration of migration) of v-eels.

	Model	AIC	Δ Deviance (%)	Corr. fitted/ observed data
American eel	Full model	1508	92.7	96.8*
	Model without swimming speed	1990	6.4	0.25*
	Model without ocean currents	1677	81.7	90.9*
	Model without behaviour	1676	81.7	90.9*
	Model without DVM range	1511	92.4	96.6*
European eel	Full model	1575	95	97.9*
	Model without swimming speed	2141	0.1	0.09 NS
	Model without behaviour	1599	94	97.4
	Model without ocean currents	1569	94.9	97.8
	Model without DVM range	1569	95	97.9

The response variable is the maximal transit time required for 95% of v-eels to reach the spawning area. For both species, the full model is: Number of days ~ Swimming speed × Ocean currents × Behaviour + DVM range. The Gaussian family and log link were applied. For both species, swimming speed is the principal factor since the explained deviance is very low when this factor is not taken into account in the model.
*$p < 0.05$.

divided by time, ranged from 17.8 to 141 km d^{-1} (Supplementary Figure S3).

The ocean currents and the type of swimming behaviours (resulting in a migratory path) significantly affect the success and duration of migration for swimming speeds <0.8 m s^{-1} (Tables 4 and 5, Figures 3 and 4). The effects of currents were particularly pronounced for American v-eels truly navigating from the Scotian Shelf to the target inside the spawning area. For both species, ocean currents increased the average duration of migration (by increasing the average total travelled distance). For instance, the duration of migration of American v-eels swimming at 0.2 m s^{-1} was increased by 11 d on average, reaching 78 d (Table 5). However, for American v-eels in both directed swimming experiments, the duration of migration declined for a certain proportion of v-eels by 1.2–39 d according to different swimming speeds, indicating that ocean currents could be favourable at some locations (Table 5). The ocean currents (e.g. the GS) increased the spatio-temporal variability of v-eels compared with the scenarios with no background ocean circulation, resulting in a clearly different distribution of the number of particles that reach the spawning area (i.e. migration success).

For both species, v-eels reached the boundaries of the spawning area earlier on average in Exp_{Ori} than in Exp_{Navi} (Figures 3 and 4, Table 3). This is mainly due to the travelled distance which is on average greater by 20.5% for American v-eels and by 12.2% for European v-eels in Exp_{Navi} (2346 km compared with 1947 km and 4960 compared with 4422 km, respectively; Supplementary Figure S4).

Our results also showed that the tested range of DVM (four combinations of four depth layers) led to very similar migration success for both v-eel species (Table 4).

Energy expenditure

The model results showed that the successful v-eels released over the Scotian Shelf spent an average of 24.5% (max of 47.7%) of the total energy available to reach the spawning site (target, Exp_{Navi}) compared with 44.6% (max of 81.3%) for the v-eels released off the Irish continental shelf (Table 3, Figure 5). The total energy expenditure is affected by the size and the swimming speed (in BL s^{-1}): it increases with the swimming speed for each given body size (Figure 5). For similar swimming speeds (in BL s^{-1}), the smallest eels spent more energy than the medium and large size eels due to a longer time for smallest eels to reach the spawning area (lower ground travel speed). For instance, at the optimal swimming speed (0.8 BL s^{-1}) and DVM range of 200–1000 m, the small American v-eels spent on average 21.3% of their available energy vs. 17.3 and 17.9% for the medium and large v-eels, respectively. Under the same conditions, the European v-eels spent on average 40.8, 30.3, and 31.8% of the total energy available, for the small, medium, and large body sizes, respectively. The behaviour, thus the migratory path, also affects the energy spent for reaching the boundaries of the spawning area. On average, American v-eels navigating towards the target (Exp_{Navi}) spent 20.5% of their total energy reserve before reaching the boundaries of the spawning area vs. 17.6% for v-eels swimming with an internal compass towards the spawning area (Exp_{Ori}) (Table 3). Similarly, European v-eels spent 40.4% of their total energy reserved in Exp_{Navi} compared with 34.7% in Exp_{Ori}.

The ocean currents affected the total amount of energy spent for migration, but mainly for the lowest swimming speed values (in BL s^{-1}; Figure 6 and Table 5). For instance, in Exp_{Navi}, medium size American v-eels swimming at 0.5 BL s^{-1} spent between 14.7 and 16.4% of their total energy without ocean currents vs. between 11.9 and 34.9% with ocean currents (Figure 6). For 46.7% of these v-eels, the energy expenditure is reduced by up to 23% and for 17.2% of them, their energy expenditure is increased by up to 53%. For European v-eels, energy expenditure is not significantly affected by the ocean circulation for the compass orientation towards the spawning area, but is for the true navigation behaviour (Figure 6, Table 5).

The depths at which v-eels are swimming also affected the total energy expenditure (Figure 6) mainly due to the effect of water temperature. V-eels swimming deeper spent less energy than eels swimming in shallower water. For example, medium-size v-eels swimming at 0.5 BL s^{-1} spent on average 15.8 and 15.0% more energy when performing DVM between 50 and 600 m than between 200 and 1000 m for American and European v-eels, respectively.

Environmental conditions experienced along the way

Oceanic currents

Currents in the surface layers (50 and 200 m) are generally much stronger, by at least a factor 2, than the currents in the deeper layers (600 and 1000 m). V-eels migrating from the Scotian Shelf experienced ocean currents approximately opposite to the currents experienced by v-eels migrating from the Irish continental shelf. Indeed, while American v-eels encountered the strongest currents

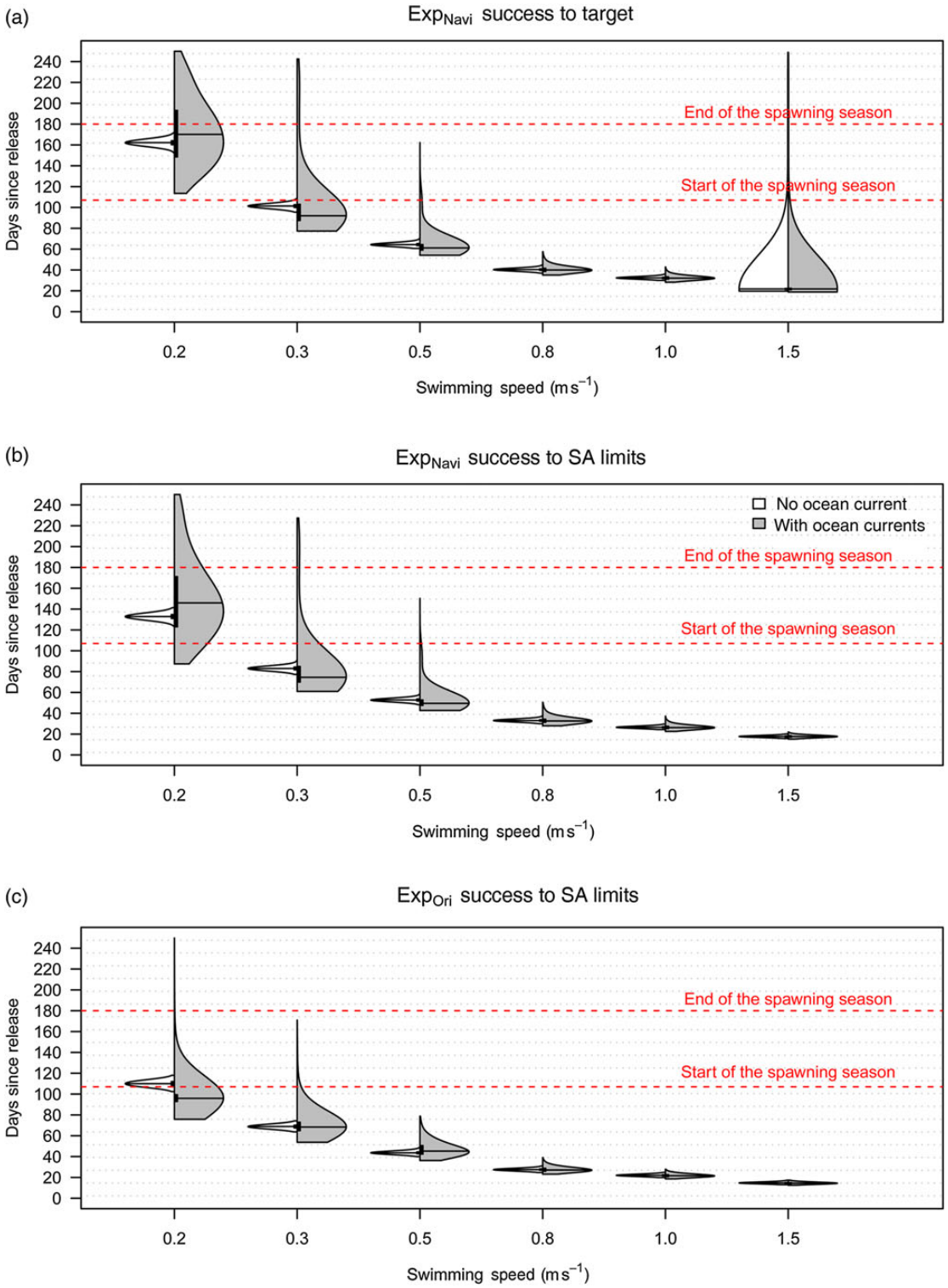

Figure 3. Distribution of the transit time of American v-eels travelling from the release site to the target inside the spawning area (SA) (a) or to the boundaries of the spawning area (b) and (c). Results according to two active behaviours and various swimming speed values are shown. Violin plots are a combination of a box plot and kernel density plot which reveals important information about the distribution of data. Horizontal expansions of the violin plots are relative to the percentage of particles that reach the spawning area. This figure is available in black and white in print and in colour at *ICES Journal of Marine Science* online.

during the first half of their journey (up to 0.7 m s^{-1}) as they cross the GS, European v-eels experienced weak currents ($<$0.1 m s^{-1}) during the first 1500 km of their journey. The strongest currents which European v-eels experienced were at around 2000 km from the northern boundary of the spawning sites in the Azores Current (Figure 1b and c). For American v-eels, the effect of the

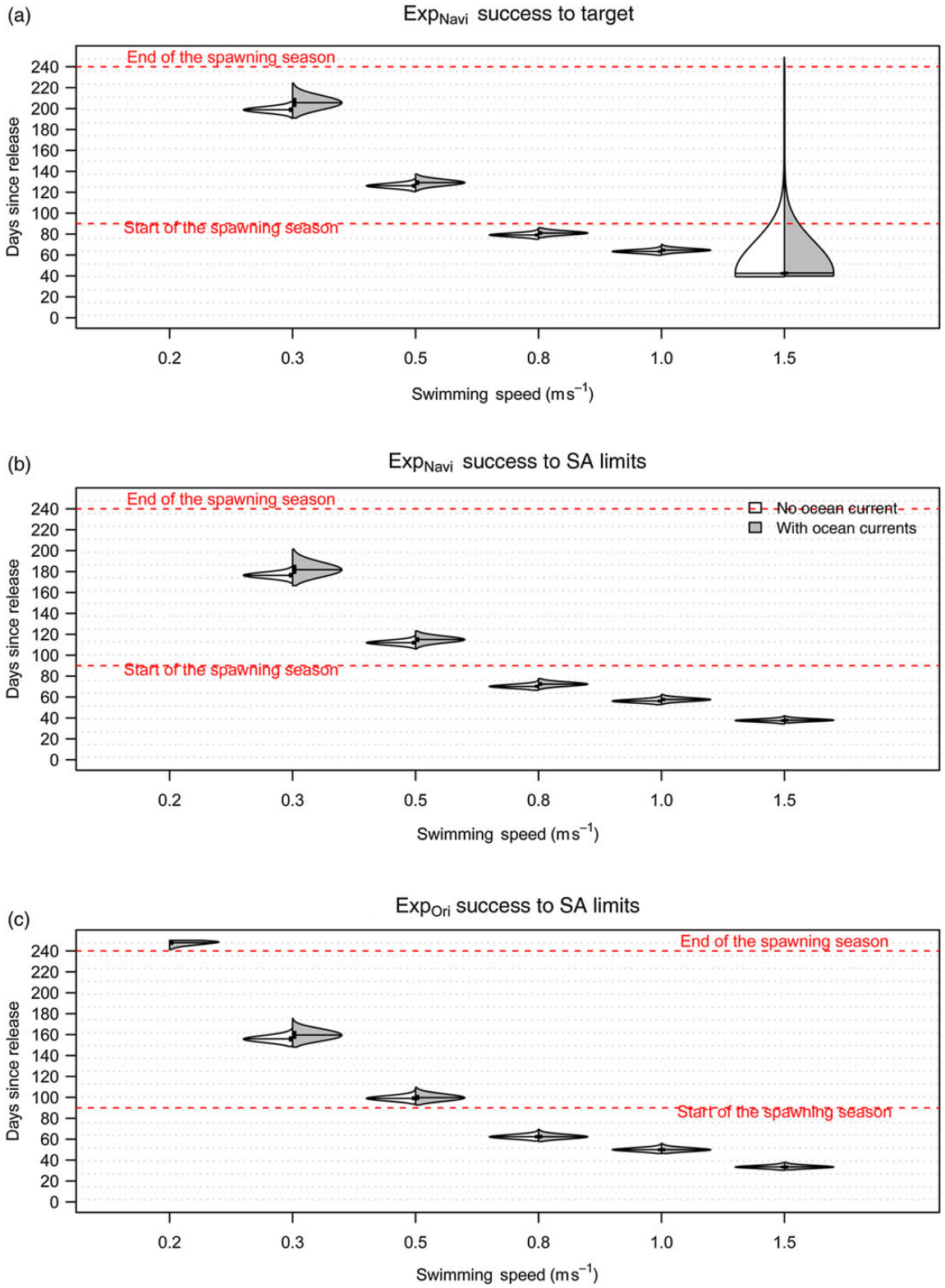

Figure 4. Distribution of the transit time of European v-eels travelling from the release site to the target inside the spawning area (SA) (a) or to the boundaries of the spawning area (b) and (c) according to two active behaviours and various swimming speed values. Otherwise as in Figure 3. This figure is available in black and white in print and in colour at *ICES Journal of Marine Science* online.

GS led to significantly different trajectories. The v-eel can be trapped in the GS rings (Figure 7b) and the v-eel could also take advantage of the strong meandering current in the GS moving towards the Sargasso Sea (Figure 7c). For individual European v-eels, the oceanic currents experienced were relatively weak, resulting in similar migratory trajectories (Figure 8).

Table 5. Summary of effects of ocean currents on the simulated spawning migration of v-eels from North America and Western Europe.

		Sws in true navigation (to target) (m s^{-1})			Sws in orientation towards Sargasso Sea (to limits of spawning area) (m s^{-1})		
Effect on	**Species**	**0.2**[a]	**0.5**	**1.0**	**0.2**[a]	**0.5**	**1.0**
Duration of migration	American v-eel	+11 d (−39 to +78 d)	+3.2 d (−6.5 to +92 d)	+0.25 d (−1.8 to +7.0 d)	+14 d (−26.6 to +131.8 d)	+1.7 d (−3.8 to +30 d)	+0.38 d (−1.2 to +3.0 d)
	European v-eel	+6.8 d (−0.1 to +17.8 d)	+3.0 d (−0.8 to +4.8 d)	+1.2 d (−0.6 to +2 d)	+3.8 d (−0.6 to +9.8 d)	+0.8 d (−0.9 to +1.9 d)	NS
Mean total travelled distance	American v-eel	+40.9% (−16.6 to +135%)	+7.3% (−33.1 to +154%)	+1.5% (−15 to +21.9%)	+15.2% (−4.6 to +79.6%)	+7.8% (−31.4 to +59.2%)	+0.7% (−13.6 to +16.6%)
	European v-eel	+2.9% (−3.3 to +8.7%)	+1.4% (−1.7 to +3.5%)	+0.7% (−0.9 to +2%)	+1.6% (−10.4 to +4.4%)	+0.8% (−0.2 to −2.5%)	NS
Total energy cost	American v-eel	+6.3% (−24.6 to +43.8%)	−0.9% (−9.8 to +11.1%)	NS	−11.2% (−23.9 to +103%)	+7.8 % (−8.2 to +71.7%)	NS
	European v-eel	+2.8% (0 to +7.1%)	+1.6 % (+0.4 to +2.2%)	NS	NS	NS	NS

Differences between average values for scenarios with ocean circulation and for those without ocean circulation are reported if statistically significant (otherwise NS is reported). Ranges are also reported: they are the difference between maximal or minimal values calculated for scenarios with and without ocean circulation. For instance: American v-eels swimming at 0.2 m s^{-1} travel on average 11 more days because of the ocean circulation, but this delay of migration can be reduced by 39 d or increased by 78 d.
[a]0.3 m s^{-1} for European eels since no v-eels were able to reach the spawning area before the end of the tracking period (250 d).

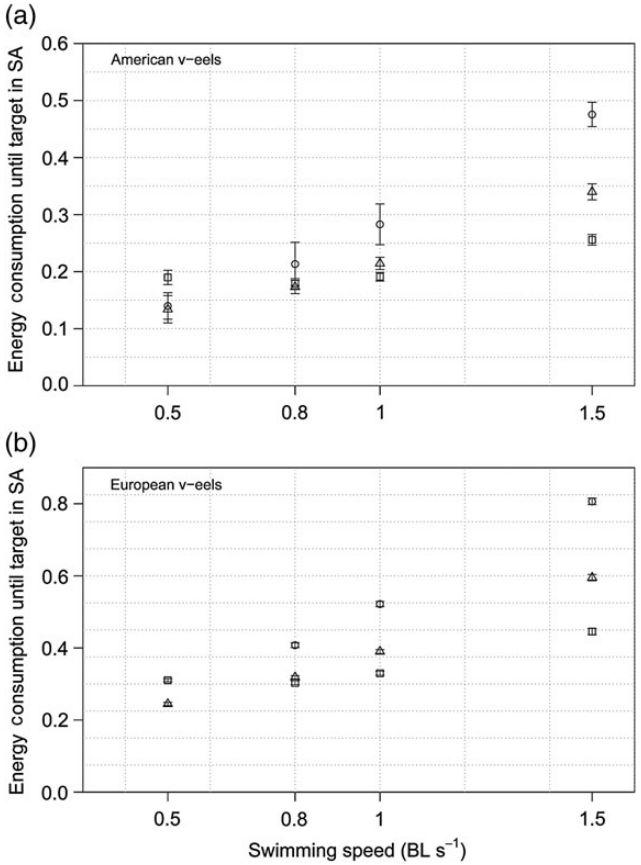

Figure 5. Percentage of available energy consumed by American v-eels (a) and European v-eels (b) at the end of their migration between coastal waters and the target inside the spawning area (SA) (Exp_{Navi}) according to various constant swimming speeds and body lengths [small v-eels (40 cm): circle; medium v-eels (64 cm): triangle; and large v-eels (102 cm): square]. The average and the standard deviation ($n = 3000$ particles for each scenario) are reported. In these scenarios, DVM of v-eels was set between 200 and 600 m.

Temperature

The use of the four depth layers in the specification of DVM led to important differences in the water temperature experienced by v-eels along their oceanic migration in all of the tested behaviours (Figure 9 and Supplementary Figure S4). For instance, a v-eel travelling from the Scotian Shelf to the Sargasso Sea at a depth of ca. 1000 m experienced a mean temperature 3.2 times colder than when travelling at ca. 50 m (mean of 21.7 vs. 6.7°C). Differences in temperature remain constant along the journey except at the beginning where the variability reached 9°C in the GS Extension region (Figure 9, Supplementary Figure S5). Similarly, a v-eel migrating from the Irish continental shelf to the Sargasso Sea at a depth of 50 m experienced a warmer water, by ca. 10°C than if travelling at 1000 m (mean of 15.3 vs. 5.4°C; Figure 9).

V-eels experienced an increasing water temperature along their migration but not in the same way between both v-species. V-eels travelling from the Irish Continental Shelf experienced a gentle temperature gradient which was ∼11 times more moderate than that experienced by v-eels travelling from the Scotian Shelf (Figure 9). Indeed, water temperature increased from ∼10–18°C at ca. 200 m depth during the first 700 km for v-eels migrating from the Scotian Shelf, representing a mean increase of 11×10^{-3}°C km^{-1}, while for the

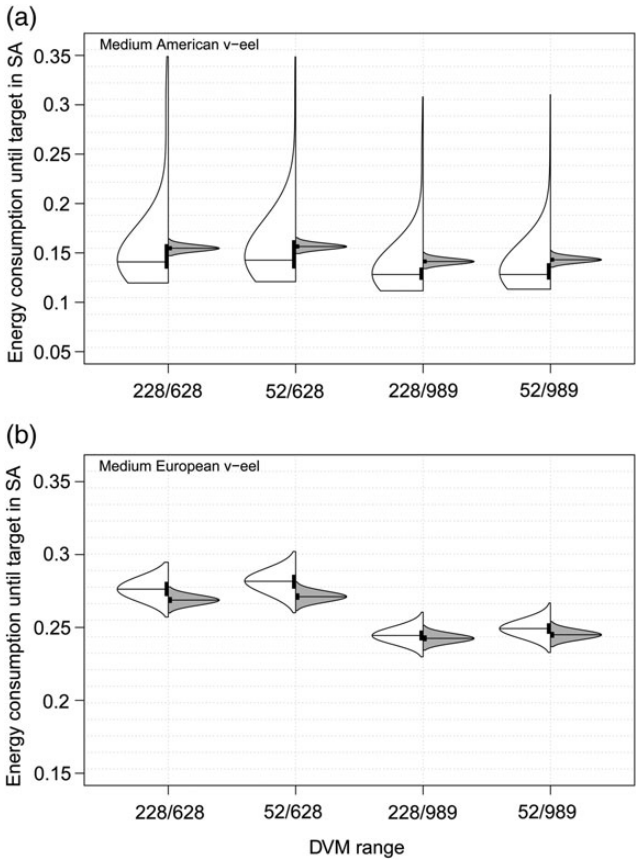

Figure 6. Mean percentage of available energy consumed by medium size American v-eels (a) and European v-eels (b) (swimming at 0.5 BL s^{-1}) at the end of their migration between coastal waters and the target inside the spawning area (SA) (Exp_{Navi}) according to the DVM range and with (grey violin plots) and without the effect of ocean currents (white violin plots). The median value of total energy consumed is marked in each violin plot.

same travelling depth, v-eels from the Irish Shelf experienced a gradient of 15×10^{-4}°C km^{-1} (11–18.5°C in more than 5000 km). For approximately the remaining two-thirds of the way for American eels, the temperature at all depth layers remained constant. For both species and for all scenarios, the temperature at ca. 50 m depth increased more rapidly at the end of the journey, due to the development of the seasonal thermocline in summer in the Sargasso Sea.

Salinity

The various depth layers occupied by v-eels led to some differences in the salinity experienced along their oceanic journey. The deepest water layers are fresher than the surface ones (Supplementary Figures S6 and S7). American v-eels experienced an increasing gradient in salinity only along the first 500 km of their migration with the salinity ranging from an average of ca. 33.6 to 36.1 at ca. 200 m deep, which represents a mean increase of 4×10^{-3} (psu) km^{-1}. European v-eels also experienced an increasing gradient of salinity, but not along the first 1000 km of their oceanic journey. At a distance of ~4000 km from the assumed spawning sites, the salinity at ca. 50 m deep progressively increased from ca. 35.4 to 36.8 at the spawning sites, which represents a gradient of 3×10^{-4} psu km^{-1}.

Discussion

A biophysical particle tracking model was used in this study for simulating the migration of American and European silver eels from the continental shelf edge to their spawning area in the Sargasso Sea.

Model results demonstrated that active-orientated swimming behaviours were required for eels to reach the Sargasso Sea. Indeed, the probability is near zero for an eel from either side of the North Atlantic Ocean to reach the spawning area in time for spawning if the eels drift with oceanic currents or swim in random directions. The model results showed that the boundaries of the spawning area can be reached by constantly swimming at the lowest swimming speed tested (0.5 BL s^{-1}, i.e. 0.2 m s^{-1} for 40-cm eels) with a readjusted heading (true navigation) or a constant heading (compass orientation). This means that the ocean currents are not strong enough to deflect eels from their final destination and true navigation may not be necessary to complete the migration.

Our results demonstrated that the ocean circulation affected significantly the migration of both v-eels species by increasing the time (or distance) to reach the spawning area, particularly for the lowest swimming speeds tested. The slower the v-eels swam, the more important was the effect of the oceanic circulation on their migration. For true navigation, a minimum constant swimming speed of 0.4 m s^{-1} for American v-eels and 0.3 m s^{-1} for European v-eels was required for 100% success of v-eels reaching the respective targets in the spawning area before the end of the spawning season. Forty-nine percent of the American v-eels constantly swimming at the lowest swimming speed (0.2 m s^{-1}) reached the spawning area before the end of the spawning season (Exp_{Navi}), whereas none of the European v-eels navigating at this minimum speed completed their migration before the end of the spawning season. One strong assumption for these scenarios was that eels swim in a continuous fashion without any pauses. This assumption seems reasonable as both males and females are able to swim continuously for 6 months in laboratory experiments (van Ginneken *et al.*, 2005; Burgerhout *et al.*, 2013a), although not at their highest swimming speed. Swimming in a continuous fashion at their critical speeds, which are ~1.5–1.6 BL s^{-1} (van Ginneken *et al.*, 2005; Burgerhout *et al.*, 2013a) however appears unlikely. Thus, eels would not reach the target in the spawning area as early as calculated by our most efficient scenario, i.e. 19 d after release for American eels and 40 d for European eels. The optimal swimming speed for eels is ~0.8 BL s^{-1} (between 0.7 and 1.0 BL s^{-1}; van den Thillart and van Ginneken, 2007; Palstra *et al.*, 2008). Almost all American eels of any size swimming at the constant optimal swimming speed would then arrive at the spawning area well in advance, i.e. 72 d on average before the beginning of the spawning season for the largest eels. The largest European eels swimming at the optimal speed would arrive on the target 14 d on average before the spawning season. The medium-size European eels would arrive 2 weeks after the beginning of the spawning season and the smallest ones, 48 d before the end of the spawning season.

The numerical results demonstrated that success of v-eels in reaching the spawning area was not significantly affected by the various combination of depths used for simulating the DVM (50/600, 50/1000, 200/600, and 200/1000 m). It should be noted that ocean currents at 600 and 1000 m are weaker than at 50 or 200 m in general over the studied regions. Swimming at greater depths will thus be more favourable, in terms of ocean circulation, to the silver eel migration. For instance, we calculated that 100% of American v-eels without DVM swimming at 0.5 m s^{-1} at 1000 m

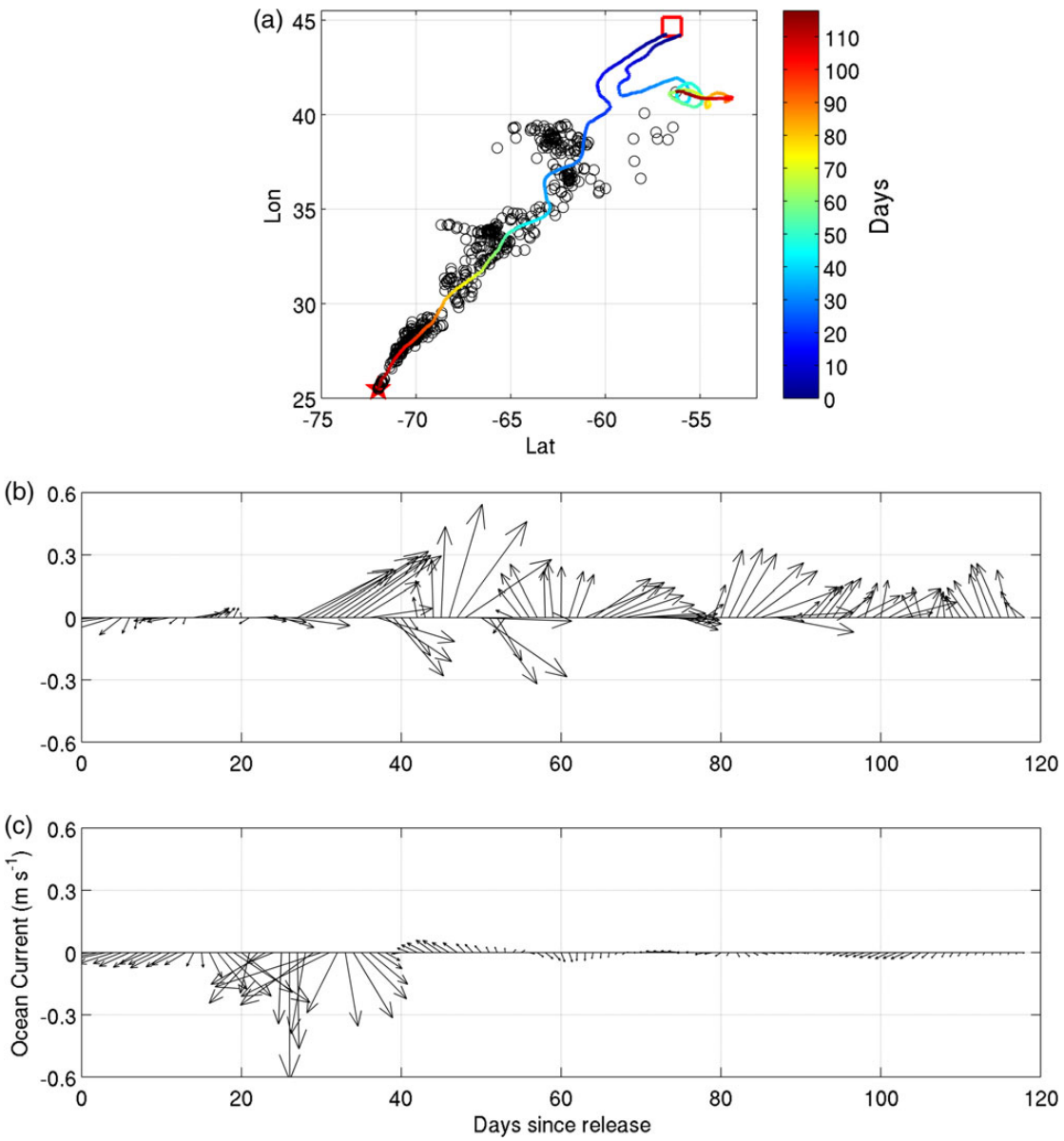

Figure 7. Trajectories (a) and ocean currents experienced by American v-eels farthest (b) and closest (c) to the target location (red star). The v-eels (BL = 404 mm, Sws = 0.5 BL s^{-1}) were released on 1 November. On day 118 since release, the first v-eel reached the target location. The locations of v-eels on day 118 are plotted as black circles along with the farthest and closest trajectories in (a). This figure is available in black and white in print and in colour at *ICES Journal of Marine Science* online.

depth will arrive within 70 d on the spawning sites compared with 163 d if swimming at 200 m depth. The temperatures at this depth (below 13°C), however, would be too cold to complete maturation. Indeed, laboratory experiments found that temperature <10°C can postpone the maturation process (Boëtius and Boëtius, 1980; van Ginneken and Maes, 2005) and the final thermal preferendum of sexually mature *Anguilla rostrata* has been established at around 17.5°C (Haro, 1991; van Ginneken and Maes, 2005). The DVM behaviour was demonstrated for many anguillids in their early marine migration (Aarestrup *et al.*, 2009; Manabe *et al.*, 2011; Beguer-Pon *et al.*, 2012; Schabetsberger *et al.*, 2013; Westerberg *et al.*, 2014), and may be a trade-off between predator avoidance and the necessity to maintain a sufficiently high metabolism for migration (e.g. Schabetsberger *et al.*, 2013).

Analysis of our numerical results demonstrated that the oceanographic conditions affect the energy expenditure of v-eels migrating at low swimming speeds to the spawning area through both currents and temperatures experienced at various depths. For true navigation, the total energy expenditure for reaching the spawning area was increased by 6.3 and 2.3% on average for slow (0.2 m s^{-1}) American and European v-eels, respectively, compared with a migration without ocean currents. The energy expenditure increase could reach 44% for American eels and 7% for European eels, but could also be reduced by 25% for American eels depending on an individual migratory path. The energy expenditures, which were previously estimated based on laboratory experiments that all considered a great-circle distance from the coasts to the Sargasso Sea (i.e. true navigation) without background oceanic currents, should thus be

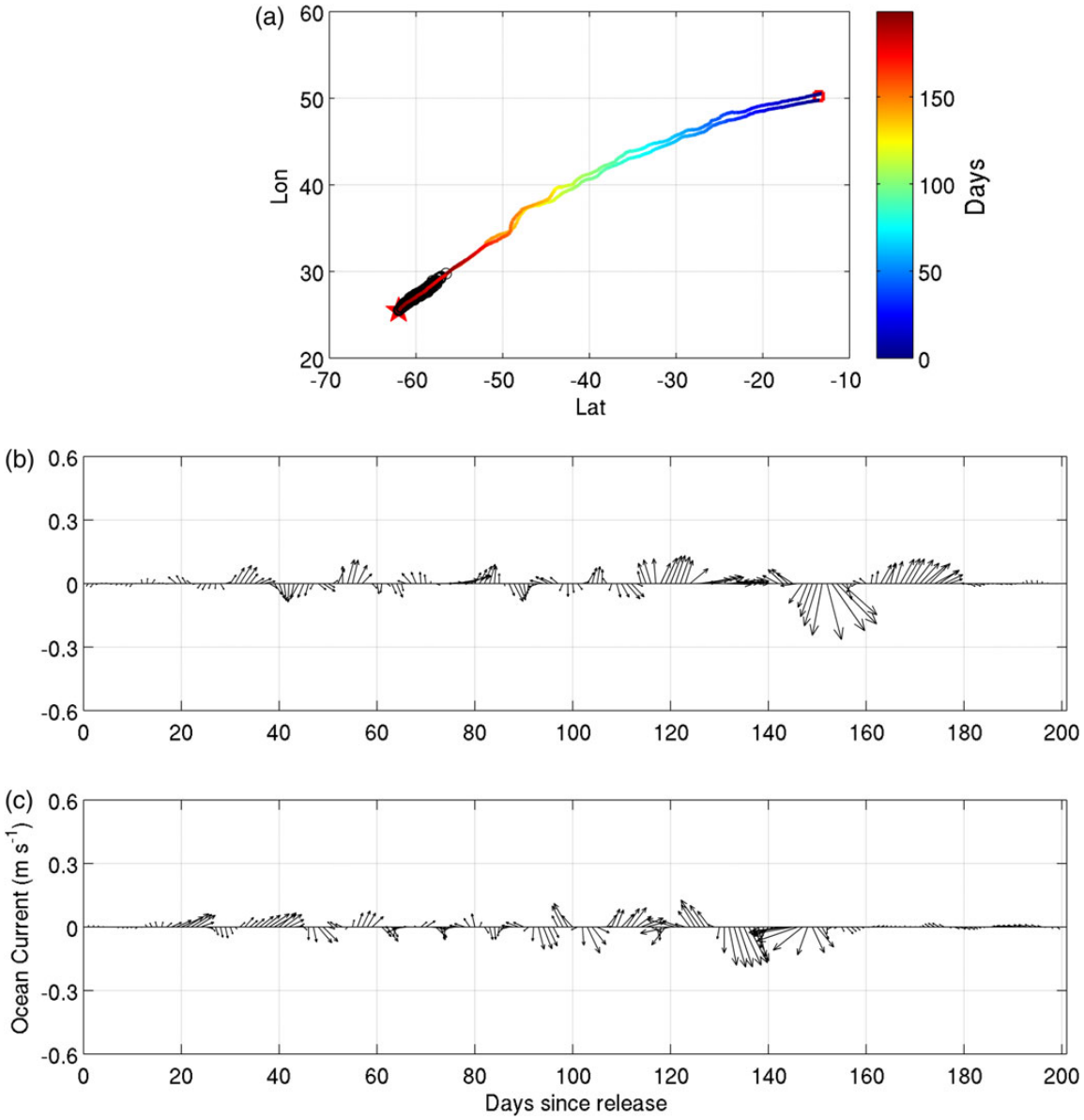

Figure 8. Trajectories (a) and ocean currents experienced by European v-eels farthest (b) and closest (c) to the target location (red star). The v-eels (BL = 637 mm, Sws = 0.5 BL s^{-1}) were released on 1 December. On day 199 since release, the first v-eel reached the target location. The locations of v-eels on day 199 are plotted as black circles along with the farthest and closest trajectories in (a). This figure is available in black and white in print and in colour at *ICES Journal of Marine Science* online.

revised upwards (energetic costs are likely underestimated; e.g. van den Thillart and van Ginneken, 2007; Palstra *et al.*, 2010; Couillard *et al.*, 2014). The energy expenditure was also affected by temperature. For instance, Walsh *et al.* (1983) showed that oxygen consumption of *A. rostrata* was increased by a factor of almost 3 when the water temperature was 20°C compared with the counterpart of 5°C. Our simulations showed that v-eels performing DVM experience vertical temperature differences as great as 15°C on their way to the Sargasso Sea from the shelf break off Nova Scotia. The difference in energy expenditure among the four depth ranges tested was on average 15% for both species. The DVM most likely occurs along the whole migratory path and its effect on energy consumption should thus be taken into account. Our model represents a valuable tool to do so.

Our simulations also indicated that energy was not a limiting factor since the maximum energy spent was 48 and 82% for American and European v-eels, respectively. A recent study on the lipid content of native and stocked American eels in Canada (Couillard *et al.*, 2014) indicated that a large proportion of native American eels would not have the necessary energy to reach the spawning sites, which is contradictory to our results. The main difference between our study and the one by Couillard *et al.* (2014) comes from the calculation of the initial reserve of energy. In our study, we took into account the total amount of lipids plus proteins (respectively, 21.1 and 16.9%), such as suggested by Palstra *et al.* (2010) who showed that the body composition stays the same during the long distance swimming of European eel. Couillard *et al.* (2014) considered only the lipid content (average of 15–

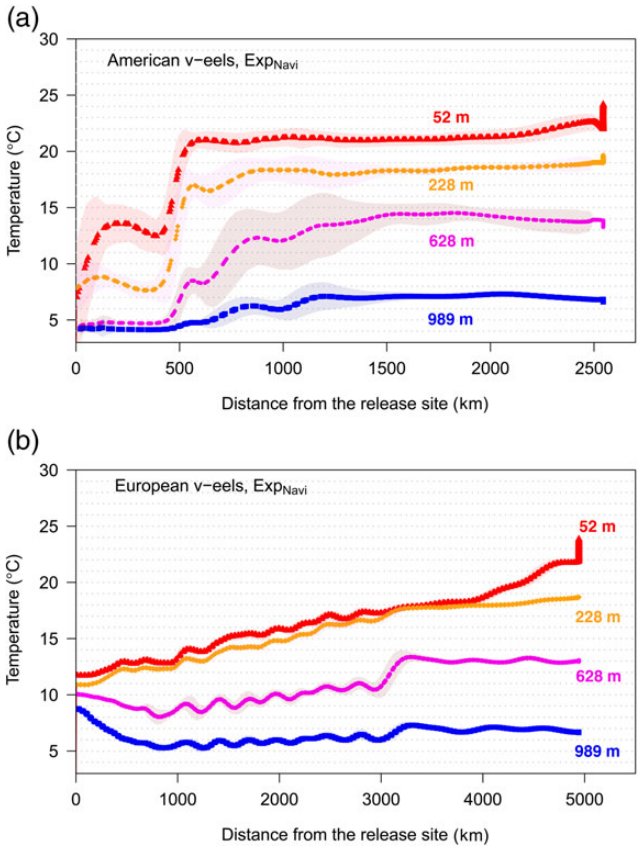

Figure 9. Mean water temperature experienced by v-eels during their migration routes with true navigation from the North American coasts (a) or from the Northwestern European coast (b) to the Sargasso Sea at various depths. In these experiments, v-eels perform DVM, but temperature profiles are represented according to depth layers for a clearer visualization. The shaded areas represent the standard deviation around the mean. The sharp decrease or increase at the end of the tracking was due mainly to the local change of temperature, particularly for the depth (52 m) close to the surface. This figure is available in black and white in print and in colour at *ICES Journal of Marine Science* online.

16%). Using their method, the initial energy reserve of our v-eels would be reduced by a factor of 2 and energy would be a limiting factor for several scenarios and particularly for European eels. We did not take into account the energetic cost due to DVM in our simulations. Simple calculations based on the additional daily travelling distance induced by this vertical behaviour indicate the total travelling distance would only be increased by $<3\%$ for both species. Performing DVM also induces additional metabolic costs required for compensating the decrease in buoyancy during the descent period (Pelster, 2015). These energetic costs remain difficult to estimate even if some rough estimates evaluate the cost to be between 7 and 22% of the energy required for swimming. It also seems that the thermal shock induced by DVM could affect oxygen consumption and thus the total energy expenditure, particularly for small eels (Trancart *et al.*, 2015). Moreover, our estimates of energy expenditure are slightly underestimated for American v-eels, particularly due to our assumption of a constant 12-h daylength in the model. Along a straight migratory path from the release locations and the spawning area, we evaluated that the daylength varies between 10 and 11.5 h, and between 9.5 and 13 h for American and European eels, respectively. In our model, American v-eels thus spend more time (1–2 h) in deeper waters, i.e. in cooler waters, than in the more complex reality. Many other factors could also affect the total energy spent during the spawning migration. For instance, Burgerhout *et al.* (2013b) recently showed that swimming in schools reduced energy consumption in male European eels. It was also demonstrated that heavy infection with the swimbladder parasite increases the costs of migration (e.g. Palstra *et al.*, 2007; Clevestam *et al.*, 2011) and it is well known that both species can be infected (e.g. Wielgoss *et al.*, 2008; Rockwell *et al.*, 2009). Furthermore, several recent studies highlighted a possible high predation rate at sea (Beguer-Pon *et al.*, 2012; Wahlberg *et al.*, 2014) and we have no idea of what amount of time and energy the eels could spend for predator avoidance.

Our simulations showed that horizontal gradients of both temperature and salinity are weak throughout most of the oceanic migration of both American and European v-eels. The spatial variation of temperature is strong in the GS region and weak in the Northwestern European shelf and the Sargasso Sea. The European v-eels experienced a constant increase in temperature of $<1 \times 10^{-3}$°C km^{-1} and a weak increase of salinity only after the first quarter of their journey (3×10^{-4} psu km^{-1}). The American v-eels experienced an increasing gradient in temperature and in salinity only during the first part of their journey (ca. 11×10^{-3}°C km^{-1} and 4×10^{-3} psu km^{-1}) and not in a consistent way (strong variability in the GS area). Freshwater fish and free-swimming marine pelagic fish demonstrate temperature discrimination of $\sim 3 \times 10^{-2}$ to 0.1°C (Bardach and Bjorklund, 1957; Steffel *et al.*, 1976) which appears inadequate for direct sensing of such weak horizontal temperature gradients calculated from our simulations. It would prevent silver eels from orientating to the horizontal temperature gradient in the open ocean. Salinity discrimination is not known but again is unlikely to provide cues for horizontal orientation.

The biophysical particle tracking model presented in this paper is a useful tool for investigating the effect of the physical marine environment on migratory behaviour and resultant pathways of American and European eels. Since the ocean migration routes of silver eels have not yet been revealed, it is difficult to conclude which behaviour is more likely to be used by eels to complete their oceanic migration. It is likely that complete spawning migration routes will be soon revealed by the ongoing field experiments and the advent of a new generation of miniature satellite tags. When migratory paths are revealed, the migratory behaviour of v-eels parameterized in the biological component of our model will be further refined (orientation mechanism, swimming speed). It will allow calculating more precise estimates of energy expenditure and migratory success, and investigating hypotheses about the observed decline of both eel species populations. Both the physical and biological components of the tracking model could also be improved in the future. Although the physical circulation model used in the study is able to capture the mean and variation of the flow field (Higginson *et al.*, 2011), the model's horizontal resolution is relatively coarse (1/4°) and the subgrid scale turbulence variability is likely to be important. The flowfields from a finer horizontal resolution model could have stronger mean currents and more small-scale features (e.g. eddies), which can lead to faster transit time and more complicated trajectories (Blanke *et al.*, 2012).

In our simulations, it should be kept in mind that we considered two specific release locations. In future work, various additional release locations will need to be considered to assess the success of both whole populations (species), which are each widely distributed

within their respective continental waters. First, size distribution of both eel species varies geographically: lengths increase with increasing latitude (and distance) from the Sargasso Sea spawning area, especially in females (Vollestad, 1992; Jessop, 2010). Size distributions are also markedly different in males and females, females being much larger than males (Vollestad, 1992; Krueger and Oliveira, 1997) and sex-ratio varying among locations (Jessop, 2010). Males inhabiting the highest latitudes will then take longer to reach the spawning area, which is very important to consider for successful spawning. Second, our model focused on migration of eels that have already reached the continental shelf edge. Depending on geographical locations, eels must first travel great distances from their growth habitat in freshwaters to reach the continental shelves, leading to longer duration of migration, lower success, and higher energetic expenditure. For instance, European eels from the edge of the North Sea migrate more than 2000 km to get to the continental shelf edge (Westerberg *et al.*, 2014), while American eels from the upper St. Lawrence River must travel an additional 1300 km from the upper St. Lawrence River to reach Cabot Strait (Béguer-Pon *et al.*, 2014) plus another 400 km to reach the shelf edge.

Supplementary data

Supplementary material is available at the *ICESJMS* online version of the manuscript.

Acknowledgements

Funding for this project was provided to JJD, MC, JS and KRT by the Ocean Tracking Network (OTN) through a network project grant (NETGP #375118-08) from the Canadian Natural Sciences and Engineering Research Council (NSERC) with additional support from the Canadian Foundation for Innovation (CFI, Project #13011). The geodetic data were kindly provided by Simon Higginson (Bedford Institute of Oceanography, NS, Canada). SS was supported by the Killam Predoctoral Fellowship. Constructive comments from three anonymous reviewers helped improve the manuscript and were greatly appreciated.

References

Aarestrup, K., Økland, F., Hansen, M. M., Righton, D., Gargan, P., Castonguay, M., Bernatchez, L., *et al.* 2009. Oceanic spawning migration of the European eel (*Anguilla anguilla*). Science, 325: 1660.

Bardach, J. E., and Bjorklund, R. G. 1957. The Temperature Sensitivity of Some American Freshwater Fishes. The American Naturalist, 91: 233–251.

Beguer-Pon, M., Benchetrit, J., Castonguay, M., Aarestrup, K., Campana, S. E., Stokesbury, M. J. W., and Dodson, J. J. 2012. Shark predation on migrating adult American eels (*Anguilla rostrata*) in the Gulf of St. Lawrence. PLoS ONE, 7: e46830.

Béguer-Pon, M., Castonguay, M., Benchetrit, J., Hatin, D., Legault, M., Verreault, G., Mailhot, Y., *et al.* 2014. Large scale migration patterns of silver American eels from the St. Lawrence River to the Gulf using acoustic telemetry. Canadian Journal of Fisheries and Aquatic Sciences, 71: 1–14.

Bilgili, A., Proehl, J. A., Lynch, D. R., Smith, K. W., and Swift, M. R. 2005. Estuary/ocean exchange and tidal mixing in a Gulf of Maine Estuary: a Lagrangian modeling study. Estuarine, Coastal and Shelf Science, 65: 607–624.

Blanke, B., Bonhommeau, S., Grima, N., and Drillet, Y. 2012. Sensitivity of advective transfer times across the North Atlantic Ocean to the temporal and spatial resolution of model velocity data: implication for European eel larval transport. Dynamics of Atmospheres and Oceans, 55–56: 22–44.

Boëtius, I., and Boëtius, J. 1980. Experimental maturation of female silver eels, *Anguilla anguilla*. Estimates of fecundity and energy reserves for migration and spawning. Dana, 1: 1–28.

Bolker, B. M., Brooks, M. E., Clark, C. J., Geange, S. W., Poulsen, J. R., Stevens, M. H. H., and White, J-S. S. 2009. Generalized linear mixed models: a practical guide for ecology and evolution. Trends in Ecology and Evolution, 24: 127–135.

Burgerhout, E., Brittijn, S. A., Tudorache, C., de Wijze, D. L., Dirks, R. P., and van den Thillart, G. E. E. J. M. 2013a. Male European eels are highly efficient long distance swimmers: effects of endurance swimming on maturation. Comparative Biochemistry and Physiology Part A: Molecular and Integrative Physiology, 166: 522–527.

Burgerhout, E., Tudorache, C., Brittijn, S. A., Palstra, A. P., Dirks, R. P., and van den Thillart, G. E. E. J. M. 2013b. Schooling reduces energy consumption in swimming male European eels, *Anguilla anguilla* L. Journal of Experimental Marine Biology and Ecology, 448: 66–71.

Chapman, J. W., Klaassen, R. H. G., Drake, V. A., Fossette, S., Hays, G. C., Metcalfe, J. D., Reynolds, A. M., *et al.* 2011. Animal orientation strategies for movement in flows. Current Biology, 21: R861–R870.

Clarke, A., and Johnston, N. M. 1999. Scaling of metabolic rate with body mass and temperature in teleost fish. Journal of Animal Ecology, 68: 893–905.

Clevestam, P. D., Ogonowski, M., Sjöberg, N. B., and Wickström, H. 2011. Too short to spawn? Implications of small body size and swimming distance on successful migration and maturation of the European eel *Anguilla anguilla*. Journal of Fish Biology, 78: 1073–1089.

COSEWIC. 2012. COSEWIC assessment and status report on the American Eel *Anguilla rostrata* in Canada. xii + 109 pp.

Couillard, C. M., Verreault, G., Dumont, P., Stanley, D., and Threader, R. W. 2014. Assessment of fat reserves adequacy in the first migrant silver American eels of a large-scale stocking experiment. North American Journal of Fisheries Management, 34: 802–813.

Davidsen, J. G., Finstad, B., ØKland, F., Thorstad, E. B., Mo, T. A., and Rikardsen, A. H. 2011. Early marine migration of European silver eel *Anguilla anguilla* in northern Norway. Journal of Fish Biology, 78: 1390–1404.

Degani, G., Gallagher, M. L., and Meltzer, A. 1989. The influence of body size and temperature on oxygen consumption of the European eel, *Anguilla anguilla*. Journal of Fish Biology, 34: 19–24.

Dodson, J. 1988. The nature and role of learning in the orientation and migratory behavior of fishes. Environmental Biology of Fishes, 23: 161–182.

Durif, C. M. F., Browman, H. I., Phillips, J. B., Skiftesvik, A. B., Vøllestad, L. A., and Stockhausen, H. H. 2013. Magnetic compass orientation in the European Eel. PLoS ONE, 8: e59212.

Elliott, J. M., and Davison, W. 1975. Energy equivalents of oxygen consumption in animal energetics. Oecologia, 19: 195–201.

Fricke, H., and Kaese, R. 1995. Tracking of artificially matured eels (*Anguilla anguilla*) in the Sargasso Sea and the problem of the eels spawning site. Naturwissenschaften, 82: 32–36.

Haro, A. J. 1991. Thermal preferenda and behavior of Atlantic eels (Genus *Anguilla*) in relation to their spawning migration. Environmental Biology of Fishes, 31: 171–184.

Helfman, G. S., Facey, D. E., Hales, S. J., and Bozeman, E. L. J. 1987. Reproductive ecology of the American eel. American Fisheries Society Symposium, 1: 42–56.

Higginson, S. 2012. Mapping and understanding the mean surface circulation of the North Atlantic: insights from new geodetic and oceanographic measurements. PhD thesis. Departement of Oceanography, Dalhousie University, Halifax. 170 pp.

Higginson, S., Thompson, K. R., Véronneau, M., Huang, J., and Wright, D. G. 2011. The mean surface circulation of the North Atlantic subpolar gyre: a comparison of estimates derived from new gravity and oceanographic measurements. Journal of Geophysical Research, 116: C08016.

IUCN. 2014. Anguilla rostrata. The IUCN Red List of Threatened Species. Version 2014.3. www.iucnredlist.org (last accessed 21 November 2014).

Jacoby, D., and Gollock, M. 2014. Anguilla anguilla. IUCN 2014. IUCN Red List of Threatened Species. Version 2014.1. www.iucnredlist.org (last accessed 2 July 2014).

Jessop, B. M. 2010. Geographic effects on American eel (*Anguilla rostrata*) life history characteristics and strategies. Canadian Journal of Fisheries and Aquatic Sciences, 67: 326–346.

Kleckner, R. C., and McCleave, J. D. 1985. Spatial and temporal distribution of American eel larvae in relation to North Atlantic Ocean current systems. Dana, 4: 67–92.

Kleiber, M. 1975. The fire of life: an introduction to animal energetics, New York, 453 pp.

Krueger, W. H., and Oliveira, K. 1997. Sex, size, and gonad morphology of silver American eels *Anguilla rostrata*. Copeia, 415–420.

Lambert, Y., and Dodson, J. J. 1990. Freshwater migration as a determinant factor in the somatic cost of reproduction of two anadromous coregonines of James Bay. Canadian Journal of Fisheries and Aquatic Sciences, 47: 318–334.

MacNamara, R., and McCarthy, T. K. 2013. Silver eel (*Anguilla anguilla*) population dynamics and production in the River Shannon, Ireland. Ecology of Freshwater Fish, 23: 181–192.

Madec, G. 2008. NEMO ocean engine. Note du Pole de modélisation, Institut Pierre-Simon Laplace (IPSL), France, No. 27. ISSN No. 1288-1619.

Manabe, R., Aoyama, J., Watanabe, K., Kawai, M., Miller, M., and Tsukamoto, K. 2011. First observations of the oceanic migration of Japanese eel from pop-up archival transmitting tags. Marine Ecology Progress Series, 437: 229–240.

McCleave, J. 2003. Spawning areas of the Atlantic eels. *In* Eel Biology, pp. 141–155. Ed. by K. Aida, K. Tsukamoto, and K. Yamauchi. Springer, Japan.

McCleave, J. D., Kleckner, R. C., and Castonguay, M. 1987. Reproductive sympatry of American and European eels and implications for migration and taxonomy. American Fisheries Society Symposium, 1: 286–297.

Methling, C., Tudorache, C., Skov, P. V., and Steffensen, J. F. 2011. Pop up satellite tags impair swimming performance and energetics of the European eel (*Anguilla anguilla*). PLoS ONE, 6: e20797.

Miller, M. J., Bonhommeau, S., Munk, P., Castonguay, M., Hanel, R., and McCleave, J. D. 2015. A century of research on the larval distributions of the Atlantic eels: a re-examination of the data. Biological Reviews. doi:10.1111/brv.12144.

Owens, S. J., and Geer, P. J. 2003. Size and age of American eels collected from tributaries of the Virginia portion of Chesapeake Bay. *In* Biology, Management, and Protection of Catadromous Eels, pp. 117–124. Ed. by D. A. Dixon. American Fisheries Society Symposium, Bethesda, MD, USA.

Palstra, A. P., Heppener, D. F. M., van Ginneken, V. J. T., Székely, C., and van den Thillart, G. E. E. J. M. 2007. Swimming performance of silver eels is severely impaired by the swim-bladder parasite *Anguillicola crassus*. Journal of Experimental Marine Biology and Ecology, 352: 244–256.

Palstra, A., van Ginneken, V., and van den Thillart, G. 2008. Cost of transport and optimal swimming speed in farmed and wild European silver eels (*Anguilla anguilla*). Comparative Biochemistry and Physiology Part A: Molecular and Integrative Physiology, 151: 37–44.

Palstra, A. P., Guido, E. E., and van den Thillart, J. M. 2010. Swimming physiology of European silver eels (*Anguilla anguilla* L.): energetic costs and effects on sexual maturation and reproduction. Fish Physiology and Biochemistry, 36: 297–322.

Palstra, A. P., Van Ginneken, V. J. T., Murk, A. J., and Van Den Thillart, G. E. E. J. M. 2006. Are dioxin-like contaminants responsible for the eel (*Anguilla anguilla*) drama? Naturwissenschaften, 93: 145–148.

Pelster, B. 2015. Swimbladder function and the spawning migration of the European eel *Anguilla anguilla*. Frontiers in Physiology, 5: 486–486.

Putman, N. F., Scanlan, M. M., Billman, E. J., O Neil, J. P., Couture, R. B., Quinn, T. P., Lohmann, K. J., *et al.* 2014. An inherited magnetic map guides ocean navigation in juvenile Pacific salmon. Current Biology, 24: 446–450.

Reid, J. L. 1994. On the total geostrophic circulation of the North Atlantic Ocean: flow patterns, tracers, and transports. Progress in Oceanography, 33: 1–92.

Ridderinkhof, H., and Zimmerman, J. T. F. 1990. Mixing processes in a numerical model of the Western Dutch Wadden Sea. *In* Residual Currents and Long-term Transport, pp. 194–209. Ed. by R. T. Chang. Springer-Verlag, New York.

Riddle, A. M., and Lewis, R. E. 2000. Dispersion Experiments in U.K. Coastal Waters. Estuarine, Coastal and Shelf Science, 51: 243–254.

Rockwell, L. S., Jones, K. M., and Cone, D. K. 2009. First record of *Anguillicoloides crassus* (Nematoda) in American eels (*Anguilla rostrata*) in Canadian estuaries, Cape Breton, Nova Scotia. The Journal of parasitology, 95: 483–486.

Rypina, I., Llopiz, J. K., Pratt, L. J., and Lozier, M. S. 2014. Dispersal pathways of American eel larvae from the Sargasso Sea. Limnology and Oceanography, 59: 1704–1714.

Schabetsberger, R., ØKland, F., Aarestrup, K., Kalfatak, D., Sichrowsky, U., Tambets, M., Dall'Olmo, G., *et al.* 2013. Oceanic migration behaviour of tropical Pacific eels from Vanuatu. Marine Ecology Progress Series, 475: 177–190.

Schmidt, J. 1923. The breeding places of the eel. Philosophical Transactions of the Royal Society of London Series B—Biological Sciences, 211: 179–208.

Schmitz, W. J., and McCartney, M. S. 1993. On the North Atlantic circulation. Reviews of Geophysics, 31: 29–49.

Shan, S., and Sheng, J. 2012. Examination of circulation, flushing time and dispersion in Halifax Harbour of Nova Scotia. Water Quality Research Journal of Canada, 47: 353–374.

Souza, J. J., Poluhowich, J. J., and Guerra, R. J. 1988. Orientation responses of American eels, *Anguilla rostrata*, to varying magnetic fields. Comparative Biochemistry and Physiology A—Physiology, 90: 57–61.

Steele, M., Morley, R., and Ermold, W. 2001. PHC: a global ocean hydrography with a high quality Arctic Ocean. Journal of Climate, 14: 2079–2087.

Steffel, S., Magnuson, J. J., Dizon, A. E., and Neill, W. H. 1976. Temperature Discrimination by Captive Free-Swimming Tuna, *Euthynnus affinis*. Transactions of the American Fisheries Society, 105: 588–591.

Talley, L. D., Pickard, G. L., Emery, W. J., and Swift, J. H. 2011. Introduction to Descriptive Physical Oceanography. Academic Press, Boston. 471 pp.

Taylor, G. 1922. Diffusion by continuous movements. Proceedings of the London Mathematical Society, s2–20: 196–212.

Tesch, F. W. 1974. Influence of geomagnetism and salinity on the directional choice of eels. Helgolander Wissenschaftliche Meeresuntersuchungen, 26: 382–395.

Tesch, F. W. 2003. The Eel. Blackwell Publishing, Oxford, UK. 408 pp.

Tesch, F. W., Wendt, T., and Karlsson, L. 1992. Influence of geomagnetism on the activity and orientation of the eel, *Anguilla anguilla* (L.), as evident from laboratory experiments. Ecology of Freshwater Fish, 1: 52–60.

Thompson, K. R., Wright, D. G., Lu, Y., and Demirov, E. 2006. A simple method for reducing seasonal bias and drift in eddy resolving ocean models. Ocean Modelling, 13: 109–125.

Trancart, T., Tudorache, C., van den Thillart, G. E. E. J. M., Acou, A., Carpentier, A., Boinet, C., Gouchet, G., *et al.* 2015. The effect of thermal shock during diel vertical migration on the energy required for oceanic migration of the European silver eel. Journal of Experimental Marine Biology and Ecology, 463: 168–172.

van den Thillart, G., and van Ginneken, V. 2007. Simulated migration of European silver eel; swim capacity and cost of transport. Journal of Marine Science and Technology, Special Issue: 1–16.

van Ginneken, V., Antonissen, E., Muller, U. K., Booms, R., Eding, E., Verreth, J., and van den Thillart, G. 2005. Eel migration to the Sargasso: remarkably high swimming efficiency and low energy costs. Journal of Experimental Biology, 208: 1329–1335.

Van Ginneken, V., and Maes, G. 2005. The European eel (*Anguilla anguilla*, Linnaeus), its lifecycle, evolution and reproduction: A literature review. Reviews in Fish Biology and Fisheries, 15: 367–398.

Verreault, G., Mingelbier, M., and Dumont, P. 2012. Spawning migration of American eel *Anguilla rostrata* from pristine (1843–1872) to contemporary (1963–1990) periods in the St Lawrence Estuary, Canada. Journal of Fish Biology, 81: 387–407.

Vollestad, L. A. 1992. Geographic variation in age and length at metamorphosis of maturing European eel—environmental effects and phenotypic plasticity. Journal of Animal Ecology, 61: 41–48.

Wahlberg, M., Westerberg, H., Aarestrup, K., Feunteun, E., Gargan, P., and Righton, D. 2014. Evidence of marine mammal predation of the European eel (*Anguilla anguilla* L.) on its marine migration. Deep Sea Research Part I: Oceanographic Research Papers, 86: 32–38.

Walsh, P. J., Foster, G. D., and Moon, T. W. 1983. The effects of temperature on metabolism of the American eel: compensation in the summer and torpor in the winter. Physiological Zoology, 56: 532–540.

Westerberg, H., Sjöberg, N. B., Lagenfelt, I., Aarestrup, K., and Righton, D. 2014. Behaviour of stocked and naturally recruited European eels during migration. Marine Ecology Progress Series, 496: 145–157.

Wielgoss, S., Taraschewski, H., Meyer, A., and Wirth, T. 2008. Population structure of the parasitic nematode *Anguillicola crassus*, an invader of declining North Atlantic eel stocks. Molecular Ecology, 17: 3478–3495.

Wysujack, K., Westerberg, H., Aarestrup, K., Trautner, J., Kurwie, T., Nagel, F., and Hanel, R. 2015. The migration behaviour of European silver eels (*Anguilla anguilla*) released in open ocean conditions. Marine and Freshwater Research, 66: 145–157.

Handling editor: Claire Paris